JOINT INSTITUTE FOR NUCLEAR RESEARCH
Dzhelepov Laboratory of Nuclear Problems
& JINR University Centre

# FINAL REPORT
## ON STAGE 1 OF THE INTERNATIONALSTUDENT PRACTICE

*“Radiation Protection and the Safety of Radiation Source” & “Pixel detector MX-10”*


**Supervisors:**
Prof. S.A. Shakour

**Students:**
1. Karriman Reda Mohamed Elsaid (Zagazig University)
2. Mohamed Hammam Sultan Nafady (MUST University)
3. Reem Ahmed Hanafy Mohamed (Cairo University)
4. Walaa Abdelrehim Sayed Mohamed (Alexandria University)


**Participation period:**
01-24 March

Dubna, 2022

## 1. Abstract

Radiation protection and the safety of radiation sources focuses on people and behavior (culture) to prevent harm to individuals when ionizing radiation or radioactive sources are being used; radiation safety focuses on system design to allow the use of hazardous equipment or materials without harming individuals and the environment. A radiation protection culture is an underlying requirement to successful implementation of radiation safety. The project aimed to provide the necessary practical skills and basic tools for those who is going to work in the field of radiation protection and the safe use of radiation sources in their countries. The project consists of a series of laboratory works on basic nuclear physics, interaction of radiation with matter, dosimetry and shielding; including BGO, LaBr3(Ce), NaI(Tl), Pixel detector MX-10, and Plastic detector. Moreover, checking their abilities to detect wide range of radioactive energy. In addition, working on Medipix detector (Medipix 1) and studying its role in medical, environmental, nuclear, high-energy physics, educational, and astronomy applications.

## 2. Introduction

For those who work with or around radiation, one of the most important factors is an awareness of the levels of radiation around them. This is primarily accomplished using radiation detectors of varying types. A basic understanding of the different types of detectors out there and how they work can go a long way both to finding the best detector for the required task and for maximizing the benefits of operating that detector. Moreover, According to International Commission of Radiation Protection ICRB the maintain the Commission's three fundamental principles of radiological protection, namely justification, optimization, and the application of dose limits, clarifying how they apply to radiation sources delivering exposure and to individuals receiving exposure [1,2].

The recent radiation technologies and their application in different sector from medical to nuclear reactors, enlighten the importance of radiation safety protocols and safety handling the radioactive sources with investing in the development of detectors with higher level of sensitivity and limited died time to detect the major portion of radioactivity and determine the next level of contamination protocols. When talking about radiation detection instruments, there are three types of detectors that are most used, depending on the specific needs of the device. These are: Gas-Filled Detectors, Scintillators, and Solid-State detectors [3.4]. Each has various strengths and weaknesses that recommend them to their own specific roles. Such as, BGO, LaBr3(Ce), NaI(Tl), and Plastic detector. In addition to, the Pixel detectors that consider an advanced detector like a digital camera consists of 3 parts: 1- Sensor (Si) 2- Electronic chip 3- USB. The size of the sensor is 1.5x1.5 cm with 256 x 256 pixels (65.536 pixel). The pixel size is 55μm x 55μm with high level of resolution and registration wide range of different types of radiation (x- ray, gamma, electron, neutron and charged particles) [5,6].

## 3. Projects Goals

1. Study radioactivity, different types of radiation sources, and detection of radiation.
2. Investigate the spectrum of alpha, beta, and gamma sources.
3. Study the attenuation of gamma radiation as a function of thickness and atomic number Z.
4. Study the shielding properties of different materials and examples of shielding calculations.
5. Learn how to calibrate a gamma scintillation spectrometer in terms of energy and activity
6. Learn how to calibrate an alpha spectrometry system in terms of energy and activity
7. Know what is meant by radiation dose and its units.
8. Portable monitors for alpha, beta, gamma radiation and determination of the background level of radiation and know methods of surveys.
9. Basic information about pixel detector.
10. Learn how to work with a pixel detector, and its set measurement parameters and evaluate their own measurements.

## 4. Scope of the Project

Radiation Protection and the Safety of Radiation Sources as well as usage of Pixel detector MX-10.

## 5. Methods

Due to different types of detectors and its properties we used, we went through different methods regrading each experiment. Such as determine resolution of each detector, determination the calibration curve, Identification of unknown source, and determination of attenuation coefficient of different shields. So, each method is explained in detail in the following sections.

## 6. Results

### 6.1. BGO Detector

#### 6.1.1. The relation between the resolution of the BGO detector and the applied voltage:

In order to get the resolution percent of a detector at a specified applied voltage, we use the following relation:

$$Resolution\ \% = \frac{\sigma}{Mean} \times 2.35 \times 100$$

We used a radioactive source, Co-60, and measured the mean and the standard deviation of the peak of the spectrum obtained from the BGO detector at a specific voltage as shown to the right for an applied voltage of 1200 V.

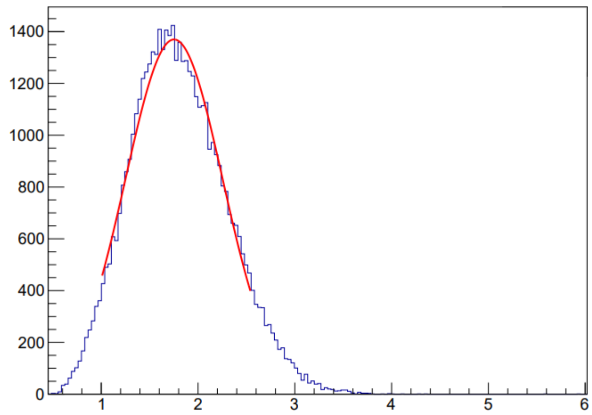


***Figure 1***:*Co-60 Spectrum at 1200 V obtained from the BGO detector*

The following experimental setup shown in Figure 2 was used.

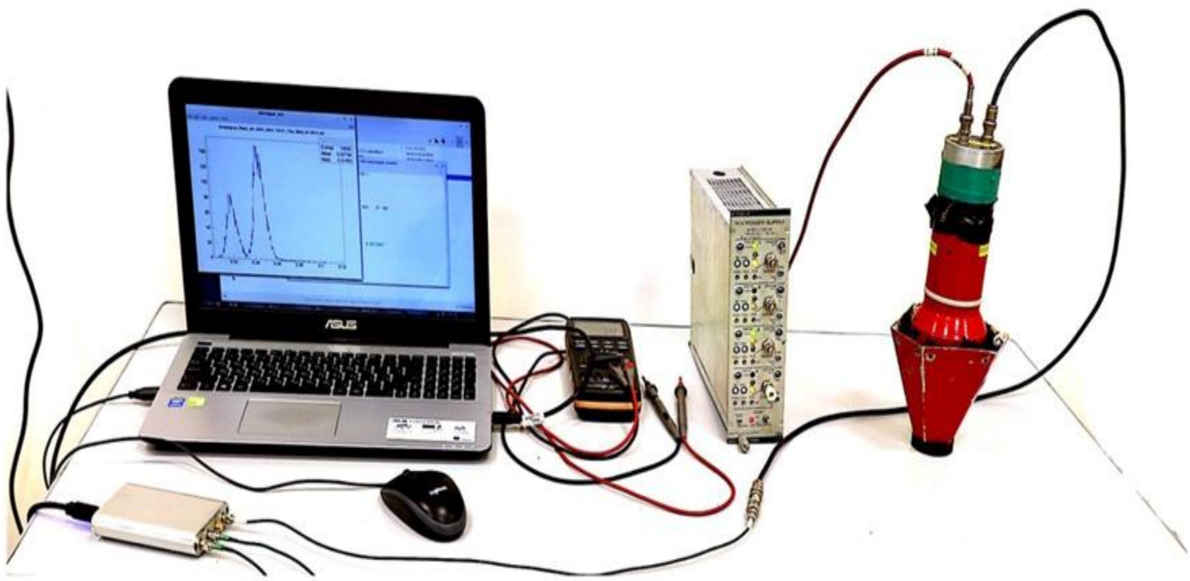

***Figure 2***. *Experimental setup for BGO detector*

It can be noted that there is an overlap of the two peaks of the Co-60 spectrum, and this is due to the bad resolution of the BGO detector at low applied voltages.

The following table shows the relation of the resolution of the BGO detector and the applied voltage.

*Table 1: The relation of the resolution of the BGO detector and the applied voltage.*

| APPLIED VOLTAGE (V) | σ | MEAN | RESOLUTION % |
|---|---|---|---|
| **1200** | 0.5089 | 1.7749 | 67.37 |
| **1300** | 0.5948 | 2.2061 | 63.36 |
| **1400** | 0.3358 | 2.1615 | 36.51 |
| **1500** | 0.2301 | 2.3889 | 22.64 |
| **1600** | 0.3197 | 3.0715 | 24.46 |
| **1700** | 0.4448 | 3.9851 | 26.23 |
| **2000** | 0.9020 | 8.2780 | 25.61 |

As the applied voltage increases, the resolution of the detector gets better.

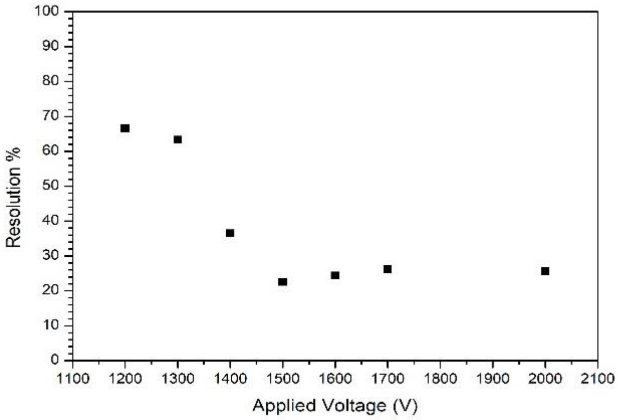


*Figure 3: The Resolution percent of the BGO detector versus the applied voltage*

### 6.1.2. Energy calibration curve of the BGO detector:

Using another radioactive source, Cs-137, at a specified voltage, 2000 V, in order to have 3 peaks with known energies to make a calibration curve as follows:

*Table 2: Energy calibration curve of the BGO detector*

| ENERGY (MEV) | PMT (A.U) |
|---|---|
| **0.662** | 5 |
| **1.25** | 8 |
| **2.5** | 16 |

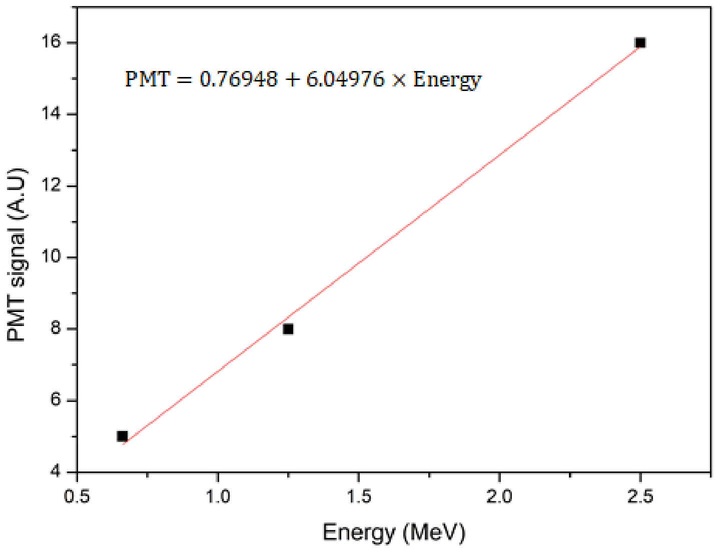


*Figure 4: Energy calibration curve of the BGO detector*

### 6.1.3. Identification of an unknown source using the energy calibration curve:

From the following spectrum of the unknown radioactive source, we obtained the value of the PMT, which is, 3.57, and substituting this value into the equation of the straight line of the latter calibration curve,

$$\text{PMT} = 0.76948 + 6.04976 \times \text{Energy}$$

we can get the energy of the unknown source which is 0.4629 MeV. Comparing this value with the values of the energies of radioactive source, we deduce that this radioactive source is Na-22 which has the energy of 511 keV. The difference in the values of the energies is mainly due to the inaccuracies in measurements.

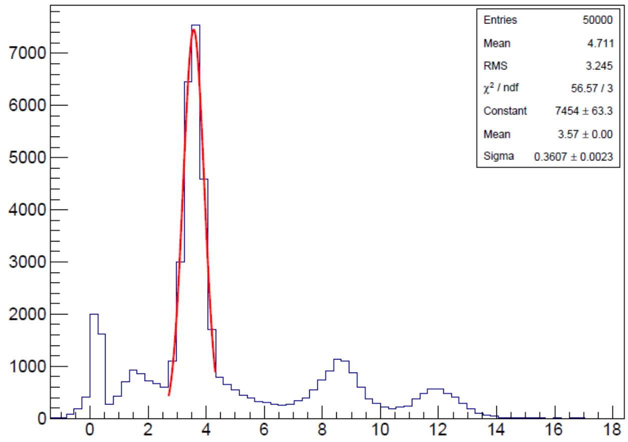


*Figure 5: Spectrum of the unknown source*

### 6.1.4. Determination of the attenuation coefficient of copper

If a beam with an initial intensity of $I_0$ passes through a material of thickness x, its intensity would drop to I as depicted in the following relation:

$$I = I_0 e^{-\mu x}$$

Where μ is the linear attenuation coefficient.

To determine the value of the attenuation coefficient of copper, a gamma radioactive source (Cs-137), the BGO detector and multiple sheets of copper with different thicknesses were used as illustrated in the following figure:

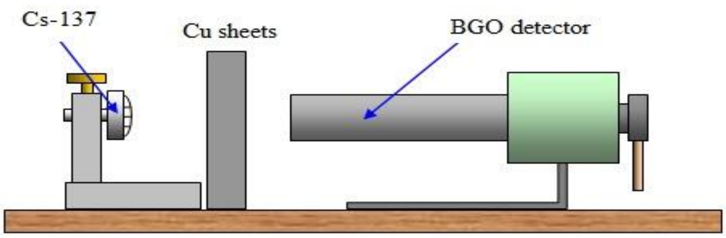


*Figure 6: Experimental set up for determination of the attenuation coefficient of copper*

The following table shows the relation between the thickness of the sheets of copper, x, measured in mm and the relative beam intensity, $\frac{I}{I_0}$, at a constant applied voltage of 2000 V.

*Table 3: The relation between the beam intensity and the thickness of the copper sheets*

| x (mm) | I (Count/s) | $\frac{I}{I_0}$ |
|---|---|---|
| **0** | 368.3513 | 1 |
| **0.5** | 363.0291 | 0.98555 |
| **1** | 359.2986 | 0.97542 |
| **1.96** | 354.3837 | 0.96208 |
| **2.46** | 351.8401 | 0.95518 |
| **2.96** | 348.0682 | 0.94494 |
| **3.92** | 345.7815 | 0.93873 |
| **4.96** | 337.6781 | 0.91673 |
| **5.96** | 334.7392 | 0.90875 |
| **8** | 327.7184 | 0.88969 |
| **10** | 318.654 | 0.86508 |
| **13.96** | 305.1013 | 0.82829 |

From the latter table, we can obtain a graph illustrating the relation between the thickness of the sheets of the copper and the relative intensities as follows:

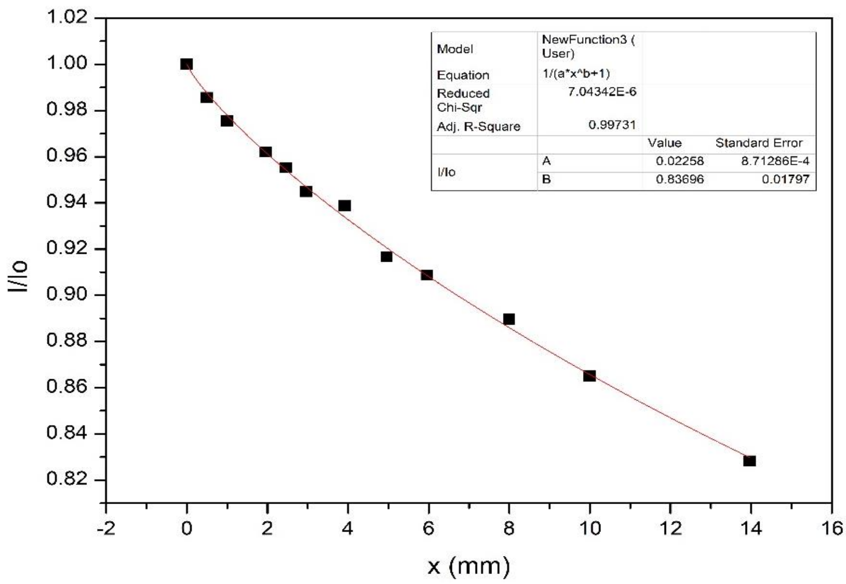


*Figure 7: Determination of the attenuation coefficient of copper.*

It can be seen that this graph verifies the equation of $I = I_0 e^{-\mu x}$ as the intensity of the beam decays exponentially with an attenuation coefficient of $\mu = 0.839\ \mathrm{mm}^{-1}$.

## 6.2. LaBr3(Ce) Detector

### 6.2.1. The relation between the resolution of the LaBr3(Ce) detector and the applied voltage:

To investigate the relation between the resolution of the LaBr3(Ce) detector and the applied voltage, a radioactive source of Co-60 was used. The same experimental set-up of the BGO detector was used but with changing the BGO detector with a LaBr3(Ce) detector.

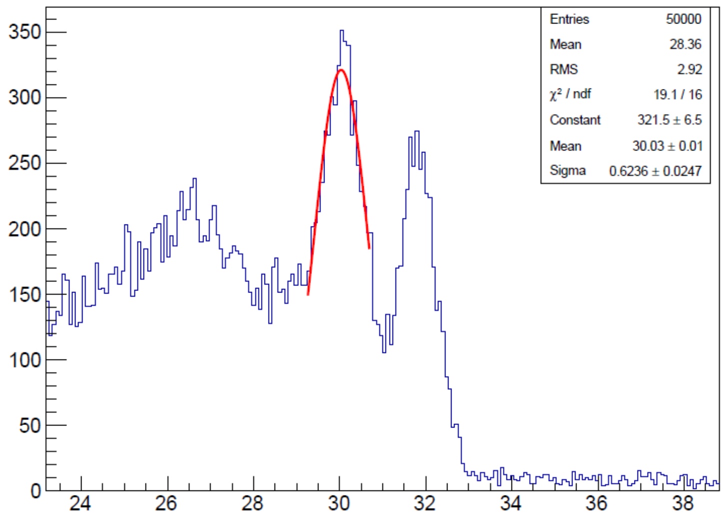


***Figure 8:*** *Spectrum of Co-60 from the LaBr3(Ce) detector at 1300 V.*

The values of the standard deviation and the mean of the first peak of the Co-60 spectrum were measured for every value of the applied voltage as can be seen in Figure 6.

The following table shows the relation between the resolution of the LaBr3(Ce) detector and the applied voltage.

***Table 4****: The relation of the resolution of the LaBr3(Ce) detector and the applied voltage.*

| APPLIED VOLTAGE (V) | σ | MEAN | RESOLUTION % |
|---|---|---|---|
| **800** | 0.2962 | 4.0342 | 17.25 |
| **900** | 0.3093 | 7.3459 | 9.89 |
| **1000** | 0.3720 | 11.6334 | 7.51 |
| **1100** | 0.4205 | 16.9239 | 5.84 |
| **1200** | 0.5682 | 23.1599 | 5.77 |
| **1300** | 0.6236 | 30.0331 | 4.88 |

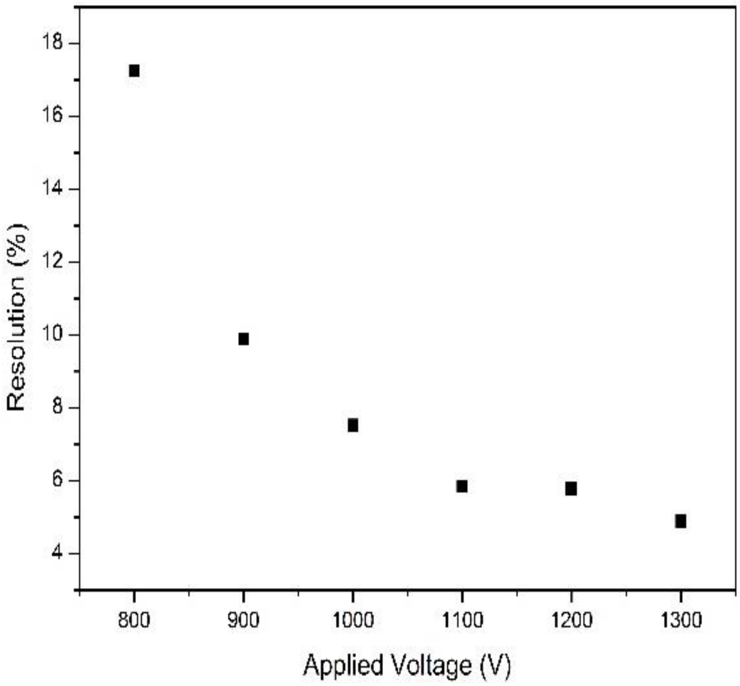


***Figure 9**: The Resolution percent of the LaBr3(Ce) detector versus the applied voltage.*

### 6.2.2. Energy calibration curve of the LaBr3(Ce) detector:

In order to obtain an energy calibration curve of the LaBr3(Ce) detector, we used the two radioactive sources, Co-60 and Cs-137, from which we obtained the following spectrum.

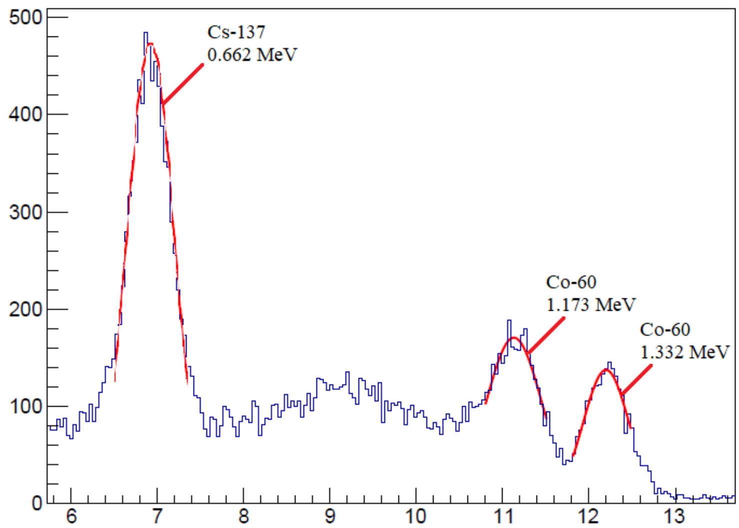


***Figure 10:** Spectrum of Co-60 and Cs-137 from the LaBr3(Ce) detector.*

From this spectrum, we have three peaks with known energies illustrated in the following table from which we can obtain an energy calibration curve of LaBr3(Ce) detector.

*Table 5: Energy calibration curve of the LaBr3(Ce) detector*

| ENERGY (MEV) | PMT (A.U) |
|---|---|
| **0.662** | 6.9094 |
| **1.173** | 11.129 |
| **1.332** | 12.1972 |

The equation of the straight line of the energy calibration curve is given by:

$$\text{PMT} = 1.65623 + 7.9769 \times \text{Energy}$$

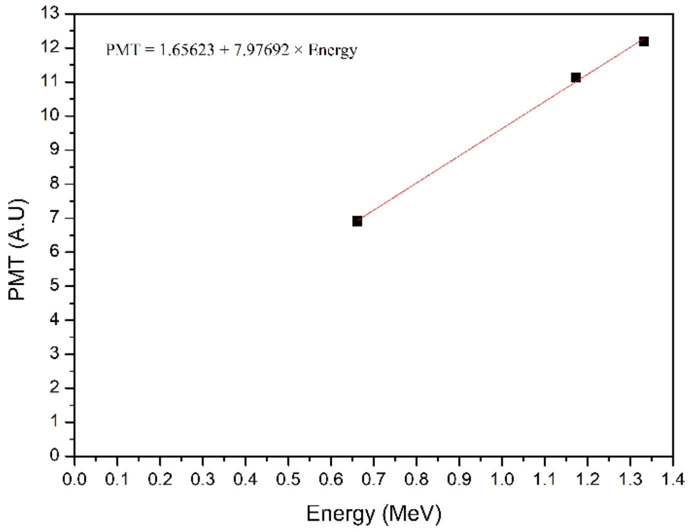


*Figure 11: Energy calibration curve of the LaBr3(Ce) detector*

This energy calibration equation can be used to identify unknown radioactive sources.

### 6.3. NaI(Tl) Detector

#### 6.3.1. The relation between the resolution of the NaI(Tl) detector and the applied voltage:

To study the resolution of the NaI(Tl) detector, a radioactive source of Co-60 was used and a similar experimental set-up of the BGO and LaBr3(Ce) detectors was used. The spectrum of the Co-60 obtained from the NaI(Tl) detector at applied voltage of 1000 V is given below.

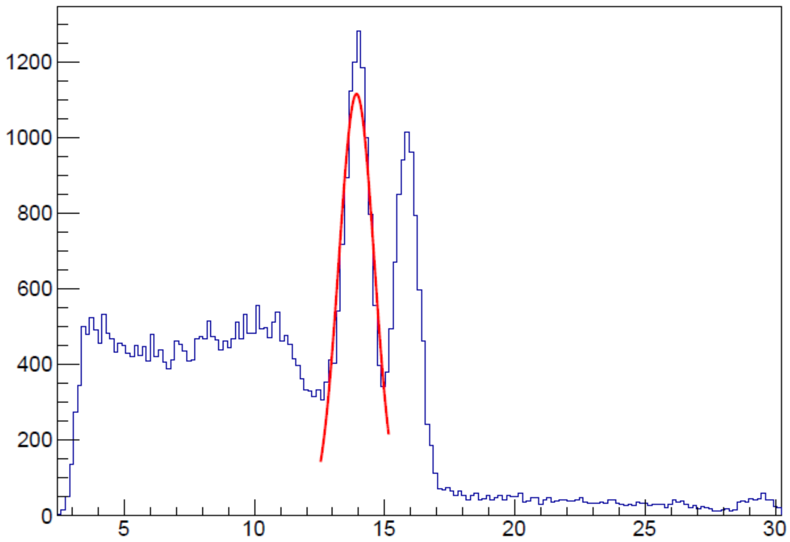

*Figure 12: Spectrum of Co-60 obtained from NaI(Tl) detector at 1000 V.*

The following table shows the relation between the resolution of the LaBr3(Ce) detector and the applied voltage.

*__Table 6:__ The relation of the resolution of the detector and the applied voltage.*

| APPLIED VOLTAGE (V) | σ | MEAN | RESOLUTION % |
|---|---|---|---|
| **1000** | 0.6792 | 13.919 | 11.467 |
| **1100** | 0.8451 | 22.9085 | 8.669 |
| **1200** | 1.4831 | 36.2407 | 9.617 |
| **1300** | 1.74479 | 55.0578 | 7.447 |
| **1400** | 2.19494 | 78.113 | 6.6035 |

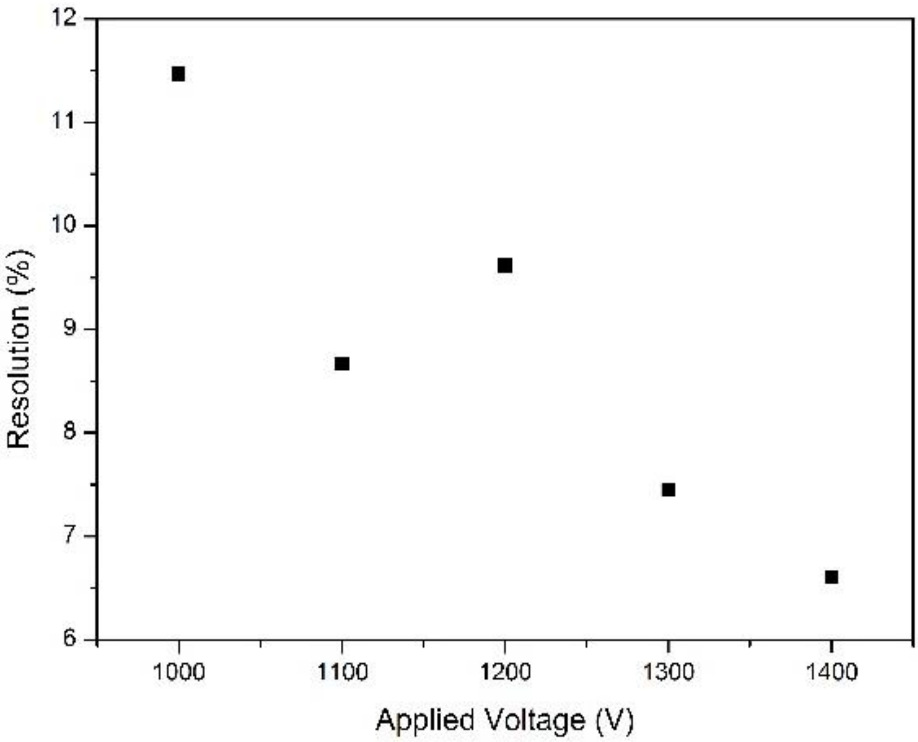


*__Figure 13:__ The Resolution percent of the NaI(Tl) detector versus the applied voltage.*

### 6.3.2. Energy calibration curve of the NaI(Tl) detector:

In order to obtain an energy calibration curve of the NaI(Tl) detector, we used the two radioactive sources, Co-60 and Cs-137, under the applied voltage of 1400V, from which we obtained the following spectrum.

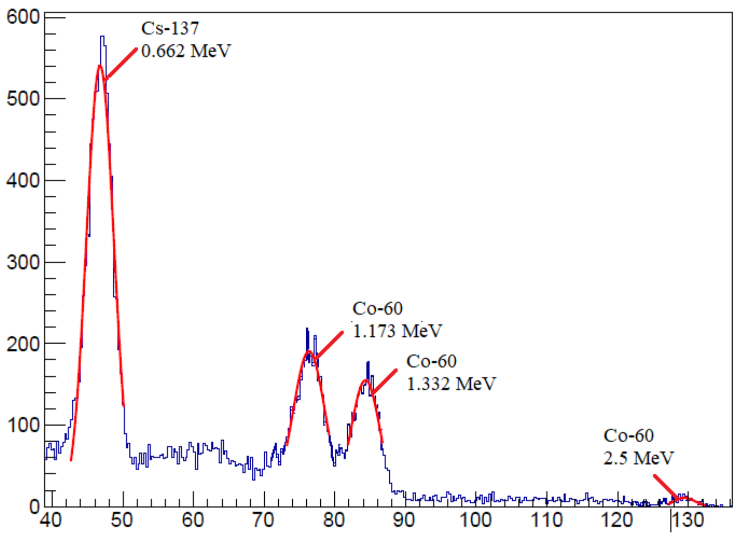


*Figure 14: Spectrum of Co-60 and Cs-137 from the NaI(Tl) detector at 1400 V*.

From this spectrum, we have four peaks with known energies illustrated in the following table from which we can obtain an energy calibration curve of NaI(Tl) detector.

*Table 7: Energy calibration curve of the NaI(Tl) detector*

| ENERGY (MEV) | PMT (A.U) |
|---|---|
| **0.662** | 46.75 |
| **1.173** | 76.36 |
| **1.332** | 84.37 |
| **2.5** | 129.5 |

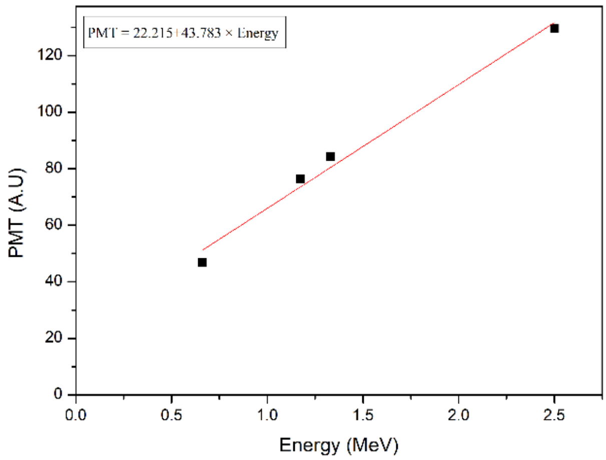


*Figure 15: Energy calibration curve of the NaI(Tl) detector*

The equation of the straight line of the energy calibration curve is given by:

$$\text{PMT} = 22.215 + 43.78312 \times \text{Energy}$$

This energy calibration relation can be used to identify unknown radioactive sources.

## 6.4. Plastic Detector

### 6.4.1. Coincidence Counting

When two particle detectors are exposed to the same radioactive source and connected to the same electronic circuit, a coincidence counting occurs. The following figure depicts the coinciding counting from two plastic detectors from a Co-60 source placed between the two detectors.


***Figure 16:*** *Coincidence counting from two plastic detectors*

The technique of coincidence counting is used to study cosmic rays which have the following spectrum.

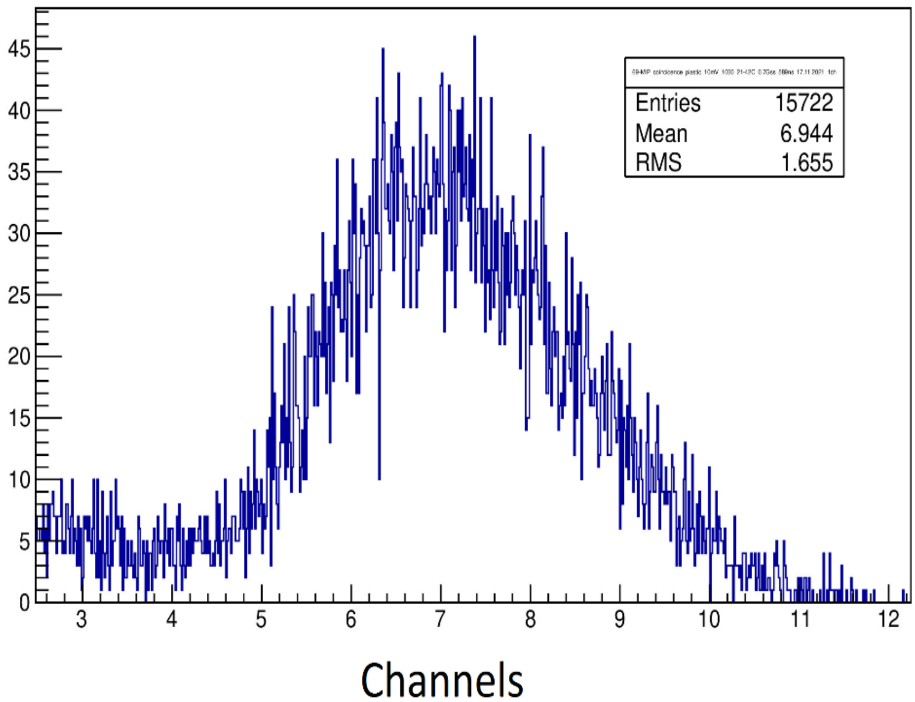


***Figure 17:*** *Registration MIP (Minimum Ionization Particle)*

From figure 17. we can see that we have two plastic detectors practically the same size and put the beam for four hours and half to registration the cosmic rays (MIP). Finally, we got coincidence spectrum energy as shown as in Figur.17.

## Under the supervision (Mr. K. Gikal, Mr. K. Papenkov)

### 6.5. Pixel Detector

#### 6.5.1. Investigating the relation between the number of particles detected by the Pixel detector and the BIAS applied

Using a uranium glass, with increasing the BIAS from 10 to 50 V with a step of 10 V, to compare the number of particles detected in each step is illustrated in the following table.

***Table 8:*** *Number of particles detected by the pixel detector at different values of BIAS*

| BIAS | ALPHA | BETA | GAMMA |
|---|---|---|---|
| **10** | 1 | 102 | 62 |
| **20** | 2 | 100 | 67 |
| **30** | 0 | 140 | 67 |
| **40** | 0 | 153 | 62 |
| **50** | 0 | 154 | 50 |

It can be easily seen from the table that the value of the BIAS increases, the number of particles detected from the uranium glass increases.

## 7. Conclusion

Studying basics in radiation protection, safety of radiation sources, and recommended radiation protection protocol. In addition to, radioactivity and naturally occurring radioactive materials Providing the necessary practical skills and basic tools for: Calculation of resolution of different scintillation detectors (BGO and NaI), Energy calibration of some scintillation detectors by using Standard sources, identification of unknown sources using the energy calibration function, determination of the attenuation coefficient, and the usage of plastic detector and pixel detector.

## 8. Acknowledgement

We want to express our great gratitude to prof said. Work under his supervision give us a great opportunity to enlightening and illustration some new technology around radiation protection and detectors developments through last decades. Additionally, we would link to thank Mr. K. Papenkov for his remarkable efforts with us.

Moreover, we would like to thank the Academy of Scientific and Technology and Joint Institute for Nuclear Research for organizing this great winter school to give us the chance to enhance our background knowledge and discover more areas of research interests.

Finally, we would like to thank our Egyptian supervisors within the winter school, University center members office, and our accommodation hotel staff members for help us and facilitate everything to enjoy our stay in Dubna, we are deeply appreciating all of your efforts with us.

## 9. References

1. Attix, F.H., Introduction to Radiological Physics and Radiation Dosimetry, Wiley, New York (1986).

2. Cember, H., Introduction to Health Physics, 3rd Edition, McGraw-Hill, New York (2000).

3. Knoll, G. F., Radiation detection and measurement, 4th Edition, Wiley (2010).

4. Martin J.E., Physics for Radiation Protection, WILEYVCH Verlag GmbH & Co. KGaA, Weinheim (2013).

5. Nuclear Radiation and Health Effects (2019). Available at: https://www.world-nuclear.org/information-library/safety-andsecurity/radiation-and-health/nuclear-radiation-and-health-effects.aspx

6. Encyclopedia Britannica (2007). Available at: https://www.britannica.com/science/coincidence-counting